AMERICAN SOCIETY FOR MICROBIOLOGY | Antimicrobial Agents and Chemotherapy®

CLINICAL THERAPEUTICS

Population Pharmacokinetics and Exposure-Response Analysis of Tribendimidine To Improve Treatment for Children with Hookworm Infection

Janneke M. Brussee,[a,b,c] Noemi Hiroshige,[a,b] Anna Neodo,[a,b] Jean T. Coulibaly,[a,b,d,e] Marc Pfister,[c,f] Jennifer Keiser[a,b]

[a]Department of Medical Parasitology and Infection Biology, Swiss Tropical and Public Health Institute, Basel, Switzerland
[b]University of Basel, Basel, Switzerland
[c]Pediatric Pharmacology and Pharmacometrics, University Children's Hospital Basel, University of Basel, Basel, Switzerland
[d]Unité de Formation et de Recherche Biosciences, Université Félix Houphouët–Boigny, Abidjan, Côte d'Ivoire
[e]Centre Suisse de Recherches Scientifiques en Côte d'Ivoire, Abidjan, Côte d'Ivoire
[f]Certara LP, Princeton, New Jersey, USA

Marc Pfister and Jennifer Keiser contributed equally.

ABSTRACT Tribendimidine has been successful in treating hookworm infections and may serve as an alternative to albendazole should resistance arise. Our aims were to (i) characterize the pharmacokinetics (PK) of tribendimidine's primary metabolite, deacetylated amidantel (dADT), and secondary metabolite, acetylated derivative of amidantel (adADT), in school-aged children and adolescents, (ii) link exposure to efficacy against hookworm, and (iii) evaluate whether tribendimidine pharmacotherapy in children could be further improved. First, a population PK model was developed based on dried-blood-spot samples collected from 155 school-aged children and adolescents with hookworm infections, following tribendimidine doses ranging from 100 to 400 mg. Second, an exposure-response analysis was conducted to link the active metabolite dADT to cure rates (CRs) and egg reduction rates (ERRs). Third, simulations were performed to identify a treatment strategy associated with >90% CRs. A two-compartmental model with transit compartments describing observed delay in absorption adequately described PK data of dADT and adADT. Allometric scaling was included to account for growth and development. The absorption rate was 56% lower with 200-mg tablets than with 50-mg tablets, while the extent of absorption remained unaffected. The identified E_{max} models linking dADT exposure to ERRs and CRs showed shallow curves, as increasing exposure led to marginal efficacy increase. Combination therapy should be considered, as a 12-fold-higher dose would be needed to achieve 95% ERRs and CRs >90% with tribendimidine alone. Further studies are warranted to evaluate safety of higher tribendimidine doses and combination therapies with other anthelmintic agents to improve treatment strategy for children with hookworm infection.

KEYWORDS tribendimidine, deacetylated amidantel, children, hookworm, pharmacokinetics, exposure-response, soil-transmitted helminths, helminthiasis, pediatric, adolescents

Helminths, parasitic worms that include the cestodes, trematodes, and nematodes, are a major public health issue in many tropical and subtropical low-income settings. Several nematode species, including the hookworms *Ancylostoma duodenale* and *Necator americanus*, are causative agents of soil-transmitted helminthiasis (STH) (1–4). Treatment of STH is highly dependent on benzimidazoles, such as albendazole and mebendazole (5), which are only moderately effective against hookworms (6). In

Citation Brussee JM, Hiroshige N, Neodo A, Coulibaly JT, Pfister M, Keiser J. 2021. Population pharmacokinetics and exposure-response analysis of tribendimidine to improve treatment for children with hookworm infection. Antimicrob Agents Chemother 65:e01778-20. https://doi.org/10.1128/AAC.01778-20.

Address correspondence to Jennifer Keiser, jennifer.keiser@swisstph.ch.

For a companion article on this topic, see https://doi.org/10.1128/AAC.00714-20.

Received 17 August 2020
Returned for modification 18 September 2020
Accepted 26 October 2020
Accepted manuscript posted online 2 November 2020
Published 20 January 2021

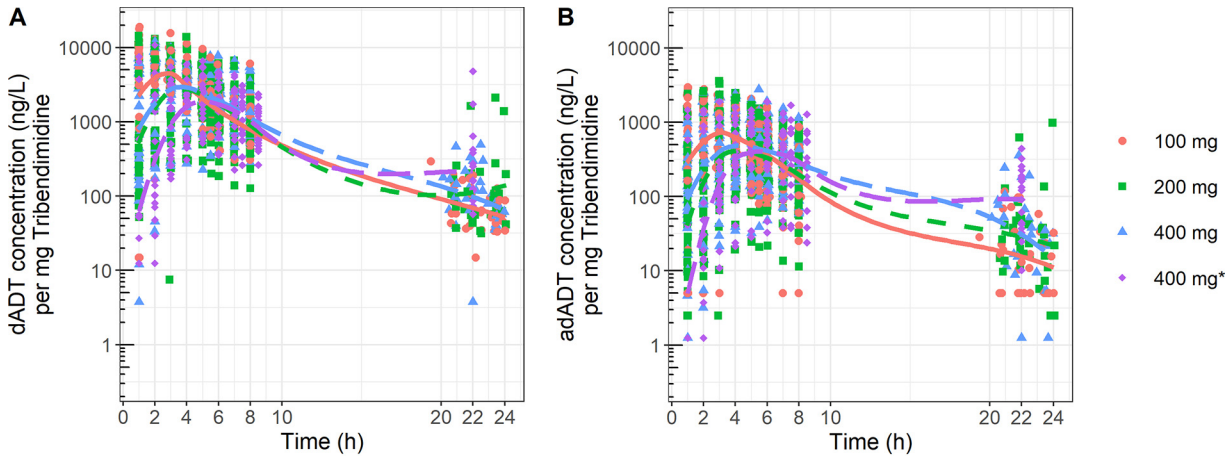

FIG 1 Dose-normalized plasma concentrations of dADT (A) and adADT (B) stratified per dose group. Colors indicate the different dose levels: red, 100 mg; green, 200 mg; blue, 400 mg in school-aged children; purple, 400 mg in adolescents (400 mg*).

addition, extensive use of only a few available drugs increases the risk of resistance (7); therefore, new therapies need to be developed for the treatment of STH (8). Achievement of cure rates (CRs) of >90% and/or egg reduction rates (ERRs) of >95% with minimal side effects by single-drug treatment have been described as the desired high-efficacy profile (9).

Tribendimidine is considered a promising and safe anthelmintic prodrug, identified and developed in China, with broad-spectrum activity against several nematodes and the liver flukes *Clonorchis sinensis* and *Opisthorchis viverrini* (10–12). Following oral administration, tribendimidine rapidly degrades to the primary metabolite deacetylated amidantel (dADT), which subsequently gets absorbed (13). The major elimination pathway is metabolism into the secondary metabolite, an acetylated derivative of amidantel (adADT), and about 35% of dADT is directly renally excreted (13). The secondary metabolite adADT is considered inactive, while tribendimidine and dADT are described to be active against hookworms *in vitro* and *in vivo* (14). CRs in adult patients receiving tribendimidine were moderate, but ERRs were high (10, 15).

So far, two population pharmacokinetic (PK) models have been developed for tribendimidine metabolites: one in *O. viverrini*-infected adolescents and adults in Laos (16) and another evaluating drug-drug interactions between anthelmintic agents in hookworm-positive adolescents in Côte d'Ivoire (17). However, a population PK model in children is lacking. Recently, a dose-ascending study in children with low infection intensities evaluated CRs and ERRs (18), and PK data were collected for a subset of this population (19). These data, combined with data from hookworm-infected adolescents, can be utilized to develop a population PK model to study the relationship between PK and outcomes (e.g., CRs and ERRs) and to simulate different dosing scenarios, thus optimizing the efficacy of tribendimidine pharmacotherapy in children.

As such, the main goals of this study were (i) to characterize PK of tribendimidine metabolites in school-aged children (6 to 12 years of age) and adolescents from Côte d'Ivoire infected with hookworm, using a population PK approach; (ii) to evaluate which exposure metrics can be predictive for efficacy against hookworms; and (iii) to identify a treatment strategy associated with >90% cure rates in children.

RESULTS

Development of the population PK model. A two-compartmental PK model best described dADT and adADT disposition in 34, 36, and 34 school-aged children receiving single doses of 100, 200, and 400 mg, respectively (19), and in 19 adolescents receiving a single dose of 400 mg tribendimidine monotherapy (17, 20). Figure 1 shows dose-normalized concentrations of dADT and adADT, stratified per dose group. Model parameters are reported in Table 1, and the model structure is shown in the supple-

TABLE 1 Parameter estimates and bootstrap results of the population PK model[a]

Parameter type	Parameter[e]	Estimate (% RSE) [% shrinkage][b]	Bootstrap median (95% CI)[c]
dADT primary metabolite			
Clearance	CL/*F* (liters/h)	57.0 (4)	56.8 (51.7–60.7)
Volume of distribution	V_C/F (liters)	259 (11)	256 (219–303)
Peripheral compartment	V_P/F (liters)	79.7 (8)	79.2 (68.1–91.4)
Intercompartmental clearance	*Q*/*F* (liters/h)	22.6 (17)	22.0 (16.3–30.4)
Absorption rate constant for 50-mg tablet (k_a) and for 200-mg tablet (*factor* ·k_a)	k_a (h^{-1})	6.36 (17)	6.62 (4.7–8.9)
	factor	0.44 (17)	0.43 (0.31–0.61)
No. of transit compartments	*N*	3.3 (17)	3.3 (2.3–4.8)
Mean transit time[d]	MTT (h) (50-mg tablet)	0.676	0.650
	MTT (h) (200-mg tablet)	1.55	1.51
Relative bioavailability	*F*	1 *fix*	1
adADT secondary metabolite			
Clearance	CL_M/F (liters/h)	235 (8)	235 (198–272)
Volume of distribution	V_{CM}/F (liters)	122 (12)	125 (98–168)
Peripheral compartment	V_{PM}/F (liters)	$=V_{CM}/F$ *fix*	
Intercompartmental clearance	Q_M/F (liters/h)	48.9 (16)	50.9 (36.4–68.9)
Interindividual variability for:			
dADT clearance	CL (ω^2)	0.10 (49) [18]	0.10 (0.03–0.31)
dADT distribution volume	V_C (ω^2)	0.78 (23) [10]	0.76 (0.40–1.18)
Absorption rate constant	k_a (ω^2)	0.42 (14) [9]	0.42 (0.31–0.59)
dADT bioavailability	*F* (ω^2)	0.077 (28) [23]	0.07 (0.04–0.12)
adADT clearance	CL_M (ω^2)	0.66 (12) [4]	0.66 (0.50–0.86)
Residual error			
Proportional error dADT		0.168 (10) [7]	0.167 (0.136–0.202)
Additive error dADT (nmol/liter)		0.005 *fix*	0.005
Proportional error adADT		0.143 (11) [8]	0.138 (0.093–0.172)
Additive error adADT (nmol/liter)		1.95 (62) [8]	2.06 (0.77–105)

[a]Population parameters are reported for a 70-kg individual and are allometrically scaled based on body weight (exponents of 0.75 and 1 for clearance and volume parameters, respectively).
[b]RSE, relative standard error. Parameters that are not estimated but fixed are indicated with "*fix*."
[c]Based on 83.4% successful runs, with the 95% CI being the 2.5th to 97.5th percentile.
[d]Mean transit time is calculated as $(N + 1)/k_{tr}$, where $k_{tr} = k_a$.
[e]*F*, relative bioavailibitlity; CL, clearance; V_c and V_p, volume of distribution of central and peripheral compartment, respectively; k_a, absorption rate constant; *N*, number of transit compartments; MTT, mean transit time. Parameters describing secondary metabolite adADT are indicated with a subscript M.

mental material (Fig. S1). To account for growth and development, allometric scaling was included, relating body weight to clearance and volume parameters with fixed exponents of 0.75 and 1, respectively. The model adequately described the data in each treatment arm, with no clear model misspecification visible in the goodness-of-fit plots (Fig. S2 and S3) and the visual predictive check (Fig. S4). Bootstrap analysis confirmed that the parameter estimates were stable and precise (Table 1).

None of the other covariates that were evaluated (dose group, age, age group, height, body mass index, coinfection with malaria, temperature, heart rate, creatinine, urea, azotemia, aspartate transaminase [AST], alanine transaminase [ALT], and bilirubin) were found to significantly correlate with any of the clearance or volume parameters. The extent of absorption (relative bioavailability) was very similar between treatment arms (Fig. 2C). In contrast, absorption rates differed significantly: for instance, the 50-mg tablets were absorbed 56% faster than the 200-mg tablets (Table 1). This affected the time for the primary metabolite to be absorbed, with mean transit times or intestinal residence times of 0.68 and 1.5 h for 50-mg and 200-mg tablets, respectively (Fig. 2A). Adolescents seemed to have a 32% slower absorption rate constant, but this was found to be insignificant ($P > 0.01$) and was therefore not included in the model. No dose-dependent clearance could be identified, indicating linear elimination (Fig. 2B). The estimated half-life of adADT was 8.7-fold lower than the estimated half-life of dADT.

A small but significant increase in relative bioavailability was identified for adolescents compared with school-aged children (Fig. 2C), but this difference was too small

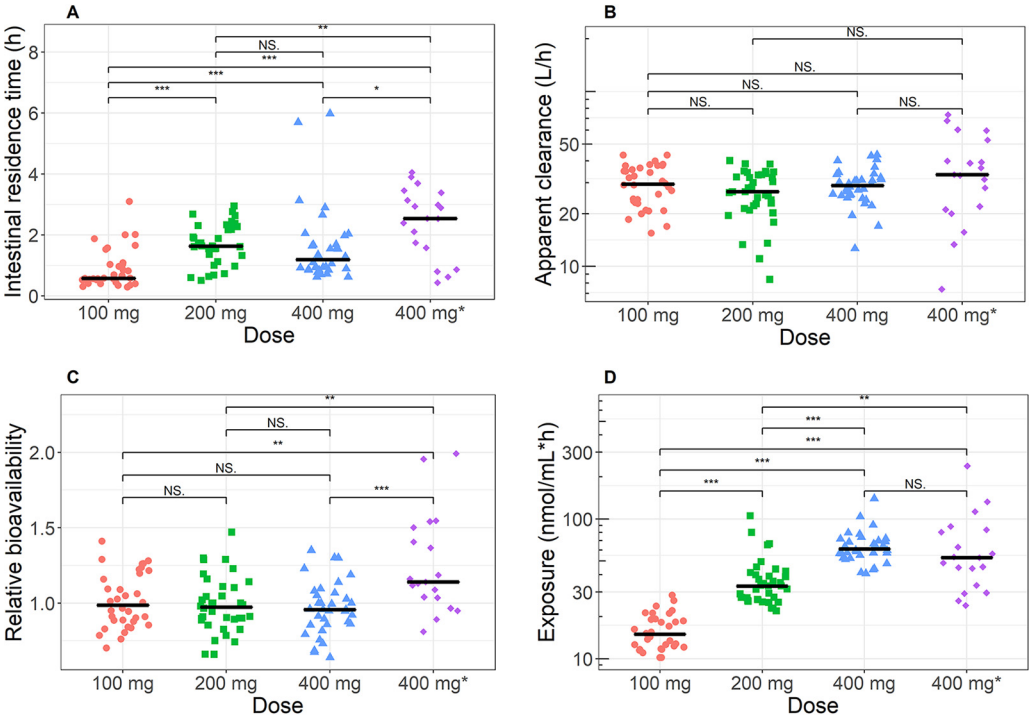

FIG 2 Pharmacokinetic parameters for primary metabolite dADT stratified per dose group, showing mean transit time (a surrogate marker for intestinal residence time) (A), apparent clearance (B), relative bioavailability (C), and total exposure ($AUC_{0-\infty}$) (D). Colors indicate the different dose levels: red, 100 mg; green, 200 mg; blue, 400 mg in school-aged children; purple, 400 mg in adolescents (400 mg*). A nonparametric test of group differences was performed using the independent 2-group Wilcoxon-Mann-Whitney test. ***, $P < 0.001$; **, $P < 0.01$; *, $P < 0.05$; NS, not significant ($P > 0.05$).

to affect the exposure (area under the curve [$AUC_{0-\infty}$]) significantly (Fig. 2D). More variability in exposure was found in adolescents (up to a 5.9-fold difference between highest and lowest exposure) than children (2.3-fold difference). Median (90% confidence interval) dADT exposure was 14.6 (11.2 to 24.8), 33.0 (22.7 to 71.0), 61.5 (42.9 to 97.2), and 53.1 (24.6 to 144.9) nmol/ml·h in the arms including 100 mg, 200 mg, and 400 mg in children and that including 400 mg in adolescents, respectively, confirming previously reported dose linearity in the 100- to 400-mg dose range (19).

Exposure-response analysis. Outcome markers (CRs and ERRs) were collected before and 14 to 21 days after treatment from all 123 school-aged children and adolescents with PK data (19, 20), as well as from 32 school-aged children receiving a placebo (18). In this population with light infections, the probability of being cured and the ERR were correlated with the exposure of the active metabolite dADT applying a maximum effect (E_{max}) model as per equations 1 and 2.

$$\text{Probability of cure} \sim \frac{E_{max} \times \text{AUC}}{E_{50} + \text{AUC}} + \text{placebo effect} \quad (1)$$

$$\text{Egg reduction rate} \sim \frac{E_{max} \times \text{AUC}}{E_{50} + \text{AUC}} + \text{placebo effect} \quad (2)$$

where CR and ERR were correlated with dADT exposure ($AUC_{0-\infty}$), a fixed maximum effect (E_{max}), and E_{50} and the placebo effect were both estimated.

The probability of being cured in the placebo group was 0.18, and the exposure associated with half the maximum effect (E_{50}) was estimated at 109.3 nmol/ml·h (Fig. 3A). The ERR in the placebo group was estimated at 31.8%, and the exposure associated with half of the maximum ERR was 68.0 nmol/ml·h (Fig. 3B). Both E_{50} values surpassed the median observed exposure following a 400-mg dose, and therefore, the correlation between dADT exposure and outcome shows shallow curves, indicating that higher exposure only slightly increases egg reduction or probability of being

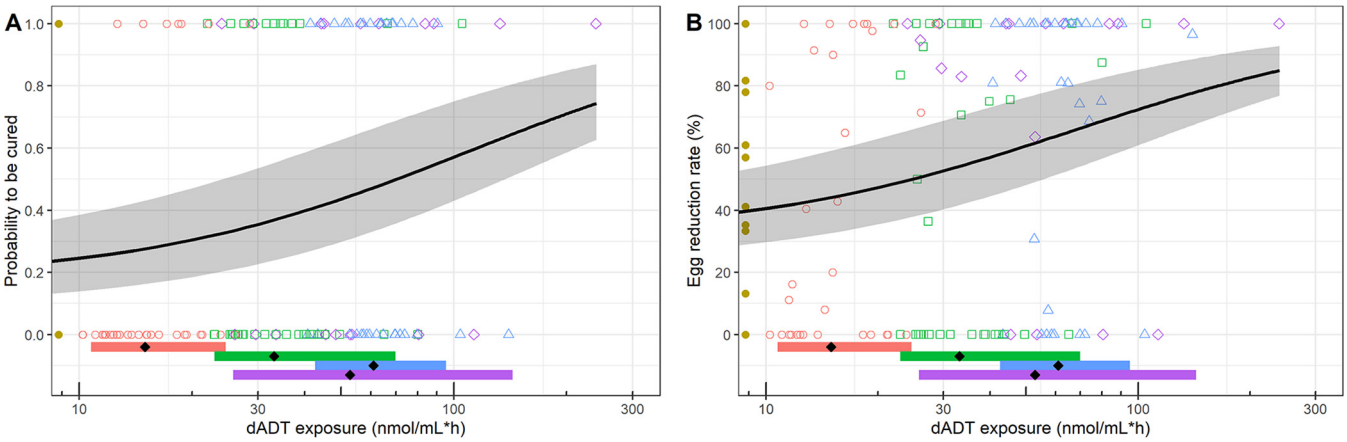

FIG 3 Exposure-response with total dADT exposure versus probability of being cured (A) and egg reduction rate (B) in children and adolescents. Colored symbols indicate individuals receiving different dose levels: yellow, placebo; red, 100 mg; green, 200 mg; blue, 400 mg in school-aged children; purple, 400 mg in adolescents. Lines indicate predicted models; shading indicates 80% confidence intervals. The horizontal colored bars show the 90% confidence interval of exposure per dose group, with the black diamonds indicating the median exposure per arm. The probability of being cured and egg reduction rate in the placebo group were estimated 0.18 and 31.8%, respectively, and the E_{50} parameters were estimated at 109.3 and 68.0 nmol/ml·h, respectively.

cured. Total dADT exposure may thus not be the best marker to predict effect, and consequently, we investigated predicted exposure in the small intestine, with the mean transit time as a surrogate marker for intestinal residence time. However, we found no significant difference in intestinal residence time between cured and noncured patients (Fig. S5).

DISCUSSION

As tribendimidine pharmacotherapy is becoming more common for treating hookworm infections in pediatric populations, it is important to understand disposition of its metabolites in children. This study presents the first population PK model for tribendimidine metabolites (dADT and adADT) in both school-aged children and adolescents. Our work fills an important knowledge gap, adding to the existing population PK models for tribendimidine metabolites in adolescents and adults in Laos infected with *O. viverrini* (16) and in adolescents in Côte d'Ivoire infected with hookworm (17).

The exposure-response analysis revealed that an increase in exposure of the active metabolite dADT correlated with a marginal gain in probability of being cured in children and adolescents with predominantly light hookworm infections. Moreover, intestinal tribendimidine residence time has been correlated with outcome, but it was not a better predictor of probability of being cured than total dADT exposure.

In the developed PK model, the estimated apparent clearance was in agreement with the previously reported parameter value obtained by noncompartmental analysis (19). Plasma clearance in our study population increased with body weight (allometric scaling) and exceeded the earlier reported values in adolescents and adults from Laos (median clearance of 57.0 liters/h (95% confidence interval [CI], 51.7 to 60.7) versus 15.8 liters/h (95% CI, 15.1 to 17.9), respectively) (16). This resulted in lower exposure and peak concentrations (C_{max}) in school-aged children and adolescents in Côte d'Ivoire following the same dose. The elimination of dADT is elimination rate limited, while the elimination of the secondary metabolite adADT is likely formation rate limited. We quantified the differences in absorption rate, with much faster absorption of the 50-mg tablets than the 200-mg tablets, which is in agreement with previously described findings (21). Interestingly, the formulation does not affect the extent of absorption, as patients receiving different tablets had similar relative bioavailabilities irrespective of the absorption rate. In adolescents, the relative bioavailability was found to be significantly higher than that in school-aged children (Fig. 2C) without leading to clinically relevant differences in exposure (Fig. 2D) due to large interindividual variability, which

ranged between 24.6 and 144.9 nmol/liter·h. A possible food effect on absorption was not studied, as all children and adolescents received a similar small local breakfast before dose administration (18–20).

The E_{max} models describe how higher exposure to the primary metabolite dADT following increasing doses is correlated with a higher probability of being cured and higher ERRs (Fig. 3). However, even 400 mg of tribendimidine fails to achieve 50% of the effect, since the median exposure at this dose (61.5 and 53.1 nmol/ml·h in school-aged children and adolescents, respectively) fell below estimated E_{50} values of 109.3 (CR) and 68.0 nmol/ml·h (ERR). The estimated E_{50} parameters in this study exceeded the previously reported 45.7 and 11.6 nmol/ml·h for adolescents. This variation might be due to the availability of data over a wider dose range (100 to 400 mg) in this study compared with a single dose level (400 mg) in the previous study (17). Alternatively, it might be attributed to difference in infection intensity, as the baseline egg count was very low in most children (18, 19), while the adolescents mostly had moderate infections (17). The estimated E_{max} models in our study were evaluated by a visual comparison to summarizing smoothing functions (Fig. S6), which showed that the model adequately described the data.

We also attempted to correlate the exposure to the secondary metabolite adADT with outcome, but it did not ameliorate the predictions of response. These results are in line with previously reported correlations between dose and response for tribendimidine (19). To the best of our knowledge, it remains unclear which PK parameter best predicts effect against hookworm, and therefore, we evaluated intestinal residence time, with mean transit time of the delayed absorption as a surrogate marker. However, the mean transit time was found not to be a good predictor, possibly because it is a function of absorption as well as rate of formation from prodrug, between which we could not differentiate based on these data. Prediction of probability of being cured could not be further improved, and thus, exposure of the primary, active metabolite dADT was utilized to correlate PK with response.

We can project doses that may reach higher treatment efficacy, assuming that the E_{max} models can be extrapolated outside the exposure range and dose linearity holds within this higher dose range. Our model-based simulations indicate that a higher dose of 4,800 mg (interquartile range [IQR], 4,000 to 5,800 mg) is necessary to obtain 90% CRs, and a similar high dose of 5,200 mg (IQR, 4,500 to 6,200 mg) is needed to achieve 95% ERRs. A previous analysis in only adolescents described similar results with elevated doses needed to achieve this desired target drug profile (17). As such exorbitant doses are unrealistic in terms of safety and practicality, and multiple administrations are inconvenient in mass drug administration programs, combination therapy with other anthelmintic agents could be considered. For instance, ivermectin and tribendimidine have shown higher efficacy against hookworm infections when coadministered (17, 20).

Limitations of our study should be acknowledged. Based on the available literature reporting studies in adults (13), we assumed that 1 mol of tribendimidine is converted completely to 2 mol of dADT, which is subsequently absorbed following a first-order process. It is then 35% renally excreted and 65% metabolized into adADT in children irrespective of age. Furthermore, since the children included in this study mostly had low-intensity hookworm infections (19), we observed only a shallow increase in efficacy with increasing exposure. This limits the power of the exposure-response analysis, and therefore, the results should be interpreted with caution. With higher-intensity infections, the correlation between dADT exposure and probability of being cured and especially ERR may be more profound. Last, to calculate a dose that achieves >90% cure and >95% egg reduction rates, we assumed dose linearity for exposure at higher doses and the possibility of extrapolating E_{max} models beyond the measured exposure range.

To conclude, a population PK model adequately described the dADT and adADT concentrations in school-aged children and adolescents following a tribendimidine dose of 100 to 400 mg. The absorption rate but not the extent depended on the tablet

formulation, with faster absorption of 50-mg tablets than 200-mg tablets. The correlation between dADT exposure and probability of being cured and ERR could be described by an E_{max} model, with only a small rise in efficacy with increasing exposure in the 100- to 400-mg dose range. To attain 90% CRs and 95% ERRs with tribendimidine monotherapy, a 12-fold-higher dose, around 4,800 mg, would be required. Therefore, to boost tribendimidine efficacy against STHs, a combination therapy with other anthelmintic drugs should be contemplated.

MATERIALS AND METHODS

Pharmacokinetic data. Patient data were combined from two previous studies: a large safety-efficacy trial of tribendimidine against hookworm infections in 130 school-aged children (18), 104 of whom gave dried-blood-spot samples (19), and 19 adolescents who received tribendimidine as monotherapy against hookworm infections in a drug-drug interaction study (20). The adolescent participants provided informed consent, and for school-aged children, the participants provided assent and their legal guardians provided informed consent. Ethical approval for both studies was obtained from the ethics committee of the Ministère de la Santé et de l'Hygiène Publique in Côte d'Ivoire (083/MSHP/CNER-kp and 053//MSHP/CNER-kp) and the ethical authorities of Switzerland (Ethikkomission Nordwest- und Zentralschweiz, reference numbers EKNZ 2017-00139 and EKNZ UBE-15/35). In addition, the study in adolescents was registered with ISRCTN (14373201).

All participants received first a local breakfast followed by treatment administration, i.e., a single dose of placebo or 100 mg, 200 mg, or 400 mg of drug, administered as a 50-mg or 200-mg tablet (Table S1) with some water. The 400-mg dose was selected because it is the highest tribendimidine dose administered in children to date. To thoroughly assess the nature of dose response of tribendimidine, the two lower doses of 100 and 200 mg were chosen in line with the available tablet formulation. Data for one individual (6 years of age) in the 400-mg group were excluded due to unrealistically low concentrations (>10-fold lower than profiles in all other studied subjects). PK samples were collected before the first dose and around 1, 2, 3, 4, 5, 5.5, 6, 7, 8, and 24 h postdose in school-aged children and around 1, 2, 3, 4, 5, 6, 7, 7.5, 8.5, and 22 h postdose in adolescents. Tribendimidine degrades rapidly to deacetylated amidantel (dADT) after oral administration, and this metabolite and the secondary metabolite, acetylated dADT (adADT), were measured in dried-blood-spot samples using a validated liquid chromatography-tandem mass spectrometry (LC-MS/MS) analysis as described elsewhere (17, 19). The lower limit of quantification (LLOQ) was 10 ng/ml in the adolescent study, while it was lower (3 and 1 ng/ml for dADT and adADT, respectively) in the school-aged-children study. All values below the LLOQ (1.1% dADT and 3.6% adADT in school-aged children and 7.2% dADT and 5.3% adADT in adolescents) were replaced by half the LLOQ, except for the measured adADT concentrations between 1 and 10 ng/ml ($n = 67$; 12.6%), which were included as reported.

Development of the PK model. (i) Structural model. A population PK model for dADT and adADT was developed utilizing nonlinear mixed-effects modeling by first-order conditional estimation with interaction (NONMEM version 7.4.1 [ICON, USA] and Pharmacometrics Modeling Workbench Pirana version 2.9.9 [Certara, USA]). Data visualization was performed in the statistical software environment R (version 3.5.1) and RStudio (version 1.1.456). It was assumed that 1 mol of tribendimidine degraded completely to 2 mol of dADT, which was subsequently absorbed following a first-order process. Estimations of lag time and transit compartments and the Sterling approximation of the number of theoretical transit compartments (22) were considered to account for the delay in absorption of dADT. For distribution of both metabolites, one-, two-, and three-compartment models were evaluated, and linear elimination was assumed for both metabolites. Furthermore, dADT was assumed to be 35% renally excreted, and a fixed percentage of 65% was assumed to be metabolized into adADT (13).

(ii) Statistical model. To account for interindividual variability in the estimated parameters, a random variable, η_i, was estimated for the ith individual from a normal distribution with a mean of zero and variance of ω^2. A lognormal distribution for the parameters in the population was assumed. To describe the residual unexplained variability, a combination of a proportional and additive error (which are each random variables from a normal distribution with a mean of zero and variance of σ^2) was included for both metabolites.

(iii) Covariate analysis. A covariate analysis was performed, where age, weight, height, body mass index, dose group, coinfection with asymptotic malaria, temperature, heart rate, tablet formulation, and the lab values for creatinine, urea, azotemia, aspartate transaminase (AST), alanine transaminase (ALT), and bilirubin were evaluated as covariates. No concomitant medications were reported. For continuous covariates, a power function with an estimated exponent correlating a normalized value to volume and clearance parameters was evaluated. Additionally, for body weight, fixed exponents of 0.75 and 1 were evaluated (allometric scaling). Categorical covariates were included by estimation of a typical value for one group compared to the other group (e.g., a covariate for a 200-mg tablet relative to a 50-mg tablet). A drop in objective function value ($-2\times$ log likelihood) by at least 6.64 points ($P < 0.01$) was considered significant for inclusion of a covariate.

(iv) Model evaluation. Nested models were compared using the objective function value. The model was evaluated with goodness-of-fit plots, including population and individual predicted versus observed concentrations, and conditionally weighted residuals versus population predictions and time after dose. To evaluate model stability and parameter precision, a bootstrap analysis using 500 resampled data sets was performed. Based on a visual predictive check (VPC) with 500

simulations, it was evaluated whether the model accurately predicts the observed concentration and the interindividual variability.

Exposure-response analysis. Study participants provided two stool samples on two consecutive days before treatment (baseline) and again at 14 to 21 days of follow-up. Hookworm egg counts (eggs per gram of stool [EPG]) were measured in these stool samples by the Kato-Katz technique (23). The difference in EPG between the baseline and follow-up samples determines the individual's ERR, which can be calculated using the following formula:

$$\mathrm{ERR} = \left[1 - \left(\mathrm{EPG}_{\mathrm{follow-up}} / \mathrm{EPG}_{\mathrm{baseline}}\right)\right] \times 100 \quad (3)$$

When no eggs are found at follow-up, a participant is considered cured. Both cure rate (CR) and ERR are considered outcome or response markers. To link PK to outcome, various E_{max} models with and without placebo effect were evaluated in a regression analysis using the non-least-squares method (R packages nls2 and nlstools). In equation 1 (see Results), the probability of being cured was correlated with dADT exposure ($AUC_{0-\infty}$). Values for E_{50} and the placebo effect were both estimated, while the maximum effect (E_{max}) was assumed to be 1 minus the placebo effect. In addition, egg reduction rates were correlated to dADT exposure, as shown in equation 2, where E_{50} and the placebo effect were estimated, while the maximum effect was assumed to be 100% minus the placebo effect (see Results). In addition, the 80% confidence interval (10th to 90th percentile) was calculated in R (version 3.5.1) and RStudio (version 1.1.456). Furthermore, we linked outcome (cured versus not cured) to intestinal exposure, utilizing mean transit time as a surrogate marker for intestinal residence time of tribendimidine and dADT.

SUPPLEMENTAL MATERIAL

Supplemental material is available online only.

SUPPLEMENTAL FILE 1, PDF file, 1.4 MB.

ACKNOWLEDGMENTS

We thank Jörg Huwyler and Maxim Puchkov for their contributions in the clinical trial.

J.K. is grateful to the ERC (CoG 614739 A-HERO) and the Swiss National Science Foundation (SNF number 320030_14930/1) for financial support. M.P. is grateful to the Eckenstein-Geigy Foundation in Basel, Switzerland, for financial support.

REFERENCES

1. Bethony J, Brooker S, Albonico M, Geiger SM, Loukas A, Diemert D, Hotez PJ. 2006. Soil-transmitted helminth infections: ascariasis, trichuriasis, and hookworm. Lancet 367:1521–1532. https://doi.org/10.1016/S0140-6736(06)68653-4.
2. Hotez PJ, Brindley PJ, Bethony JM, King CH, Pearce EJ, Jacobson J. 2008. Helminth infections: the great neglected tropical diseases. J Clin Invest 118:1311–1321. https://doi.org/10.1172/JCI34261.
3. Pullan RL, Brooker SJ. 2012. The global limits and population at risk of soil-transmitted helminth infections in 2010. Parasit Vectors 5:81. https://doi.org/10.1186/1756-3305-5-81.
4. Loukas A, Hotez PJ, Diemert D, Yazdanbakhsh M, McCarthy JS, Correa-Oliveira R, Croese J, Bethony JM. 2016. Hookworm infection. Nat Rev Dis Primers 2:16088. https://doi.org/10.1038/nrdp.2016.88.
5. Keiser J, Utzinger J. 2010. The drugs we have and the drugs we need against major helminth infections. Adv Parasitol 73:197–230. https://doi.org/10.1016/S0065-308X(10)73008-6.
6. Moser W, Schindler C, Keiser J. 2017. Efficacy of recommended drugs against soil transmitted helminths: systematic review and network meta-analysis. BMJ 358:j4307. https://doi.org/10.1136/bmj.j4307.
7. EMA Committee for Medicinal Products for Veterinary Use. 2017. Reflection paper on anthelmintic resistance. EMA/CVMP/EWP/573536/2013.
8. Hotez PJ. 2017. Global deworming: moving past albendazole and mebendazole. Lancet Infect Dis 17:1101–1102. https://doi.org/10.1016/S1473-3099(17)30484-X.
9. Olliaro P, Seiler J, Kuesel A, Horton J, Clark JN, Don R, Keiser J. 2011. Potential drug development candidates for human soil-transmitted helminthiases. PLoS Negl Trop Dis 5:e1138. https://doi.org/10.1371/journal.pntd.0001138.
10. Xiao SH, Utzinger J, Tanner M, Keiser J, Xue J. 2013. Advances with the Chinese anthelminthic drug tribendimidine in clinical trials and laboratory investigations. Acta Trop 126:115–126. https://doi.org/10.1016/j.actatropica.2013.01.009.
11. Xiao SH, Hui-Ming W, Tanner M, Utzinger J, Chong W. 2005. Tribendimidine: a promising, safe and broad-spectrum anthelmintic agent from China. Acta Trop 94:1–14. https://doi.org/10.1016/j.actatropica.2005.01.013.
12. Kulke D, Krucken J, Harder A, von Samson-Himmelstjerna G. 2014. Efficacy of cyclooctadepsipeptides and aminophenylamidines against larval, immature and mature adult stages of a parasitologically characterized trichurosis model in mice. PLoS Negl Trop Dis 8:e2698. https://doi.org/10.1371/journal.pntd.0002698.
13. Yuan G, Xu J, Qu T, Wang B, Zhang R, Wei C, Guo R. 2010. Metabolism and disposition of tribendimidine and its metabolites in healthy Chinese volunteers. Drugs R D 10:83–90. https://doi.org/10.2165/11539320-000000000-00000.
14. Tritten L, Nwosu U, Vargas M, Keiser J. 2012. In vitro and in vivo efficacy of tribendimidine and its metabolites alone and in combination against the hookworms *Heligmosomoides bakeri* and *Ancylostoma ceylanicum*. Acta Trop 122:101–107. https://doi.org/10.1016/j.actatropica.2011.12.008.
15. Steinmann P, Zhou XN, Du ZW, Jiang JY, Xiao SH, Wu ZX, Zhou H, Utzinger J. 2008. Tribendimidine and albendazole for treating soil-transmitted helminths, *Strongyloides stercoralis* and *Taenia* spp.: open-label randomized trial. PLoS Negl Trop Dis 2:e322. https://doi.org/10.1371/journal.pntd.0000322.
16. Meister I, Assawasuwannakit P, Vanobberghen F, Penny MA, Odermatt P, Sayasone S, Huwyler J, Tarning J, Keiser J. 2019. Pooled population pharmacokinetic analysis of tribendimidine for the treatment of *Opisthorchis viverrini* infections. Antimicrob Agents Chemother 63:e01391-18. https://doi.org/10.1128/AAC.01391-18.
17. Brussee JM, Neodo A, Schulz JD, Coulibaly JT, Pfister M, Keiser J. 2021. Pharmacometric analysis of tribendimidine monotherapy and combination therapies to achieve high cure rates in patients with hookworm infections. Antimicrob Agents Chemother 65:e00714-20. https://doi.org/10.1128/AAC.00714-20.
18. Coulibaly JT, Hiroshige N, N'Gbesso YK, Hattendorf J, Keiser J. 2019. Efficacy and safety of ascending dosages of tribendimidine against hookworm infections in children: a randomized controlled trial. Clin Infect Dis 69:845–852. https://doi.org/10.1093/cid/ciy999.
19. Hiroshige N, Coulibaly J, Huwyler J, Bonate PL, Keiser J. 2018. Pharmacokinetics of a pediatric tribendimidine dose-finding study to treat

hookworm infection in African children. Antimicrob Agents Chemother 62:e00959-18. https://doi.org/10.1128/AAC.00959-18.
20. Moser W, Coulibaly JT, Ali SM, Ame SM, Amour AK, Yapi RB, Albonico M, Puchkov M, Huwyler J, Hattendorf J, Keiser J. 2017. Efficacy and safety of tribendimidine, tribendimidine plus ivermectin, tribendimidine plus oxantel pamoate, and albendazole plus oxantel pamoate against hookworm and concomitant soil-transmitted helminth infections in Tanzania and Cote d'Ivoire: a randomised, controlled, single-blinded, non-inferiority trial. Lancet Infect Dis 17:1162–1171. https://doi.org/10.1016/S1473-3099(17)30487-5.
21. Duthaler U, Sayasone S, Vanobbergen F, Penny MA, Odermatt P, Huwyler J, Keiser J. 2016. Single-ascending-dose pharmacokinetic study of tribendimidine in *Opisthorchis viverrini*-infected patients. Antimicrob Agents Chemother 60:5705–5715. https://doi.org/10.1128/AAC.00992-16.
22. Savic RM, Jonker DM, Kerbusch T, Karlsson MO. 2007. Implementation of a transit compartment model for describing drug absorption in pharmacokinetic studies. J Pharmacokinet Pharmacodyn 34:711–726. https://doi.org/10.1007/s10928-007-9066-0.
23. Tarafder MR, Carabin H, Joseph L, Balolong E, Jr, Olveda R, McGarvey ST. 2010. Estimating the sensitivity and specificity of Kato-Katz stool examination technique for detection of hookworms, *Ascaris lumbricoides* and *Trichuris trichiura* infections in humans in the absence of a 'gold standard'. Int J Parasitol 40:399–404. https://doi.org/10.1016/j.ijpara.2009.09.003.